

**Hybrid noble-metals/metal-oxide bifunctional nano-heterostructure displaying  
outperforming gas-sensing and photochromic performances**

David Maria Tobaldi,<sup>a\*</sup> Salvatore Gianluca Leonardi,<sup>b</sup> Kaveh Movlaee,<sup>b,c</sup> Luc Lajaunie,<sup>d</sup> Maria Paula Seabra,<sup>a</sup>  
Raul Arenal,<sup>d,e</sup> Giovanni Neri,<sup>b</sup> João António Labrincha<sup>a</sup>

<sup>a</sup> Department of Materials and Ceramics Engineering/CICECO–Aveiro Institute of Materials, University of Aveiro,  
Campus Universitário de Santiago, 3810-193 Aveiro, Portugal

<sup>b</sup> Department of Engineering, University of Messina, C.da Di Dio, 98166 Messina, Italy

<sup>c</sup> Center of Excellence in Electrochemistry, School of Chemistry, College of Science, University of Tehran, 14155-6455  
Tehran, Iran

<sup>d</sup> Laboratorio de Microscopías Avanzadas, Instituto de Nanociencia de Aragón, Universidad de Zaragoza, 50018  
Zaragoza, Spain

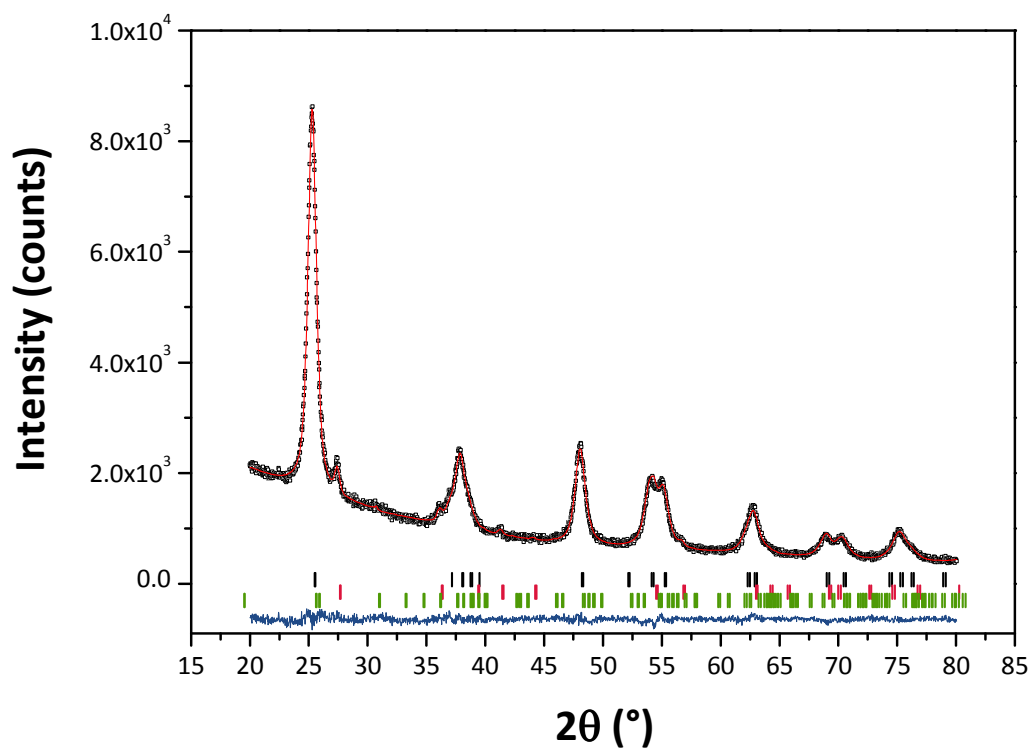
<sup>e</sup> ARAID Foundation, 50018 Zaragoza, Spain

\*Corresponding author. Tel.: +351 234 370 041

E-mail addresses: [david.tobaldi@ua.pt](mailto:david.tobaldi@ua.pt); [david@davidtobaldi.org](mailto:david@davidtobaldi.org) (DM Tobaldi)

*Supplementary Information File*

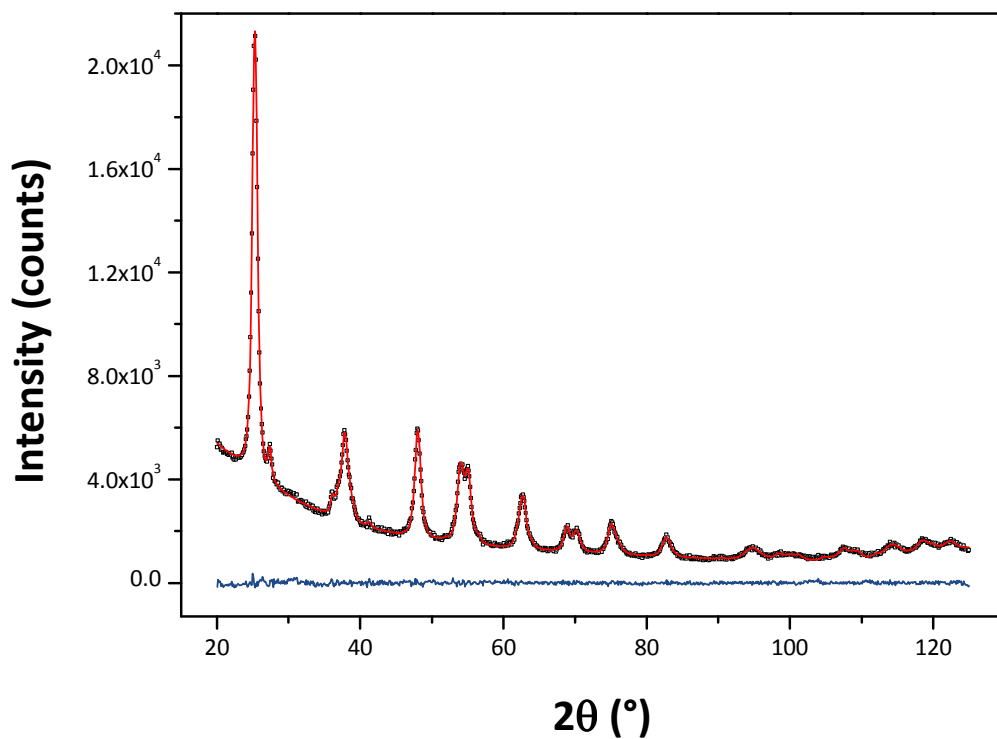
Figure S1



Graphic output of the Rietveld refinement of the sample **SBC1**. The red line represents the calculated pattern, the black open squares represent the observed pattern, and the difference curve between observed and calculated profiles is plotted below. The position of reflections is indicated by the small vertical bars (black: anatase; red: rutile; green: brookite).

*Supplementary Information File*

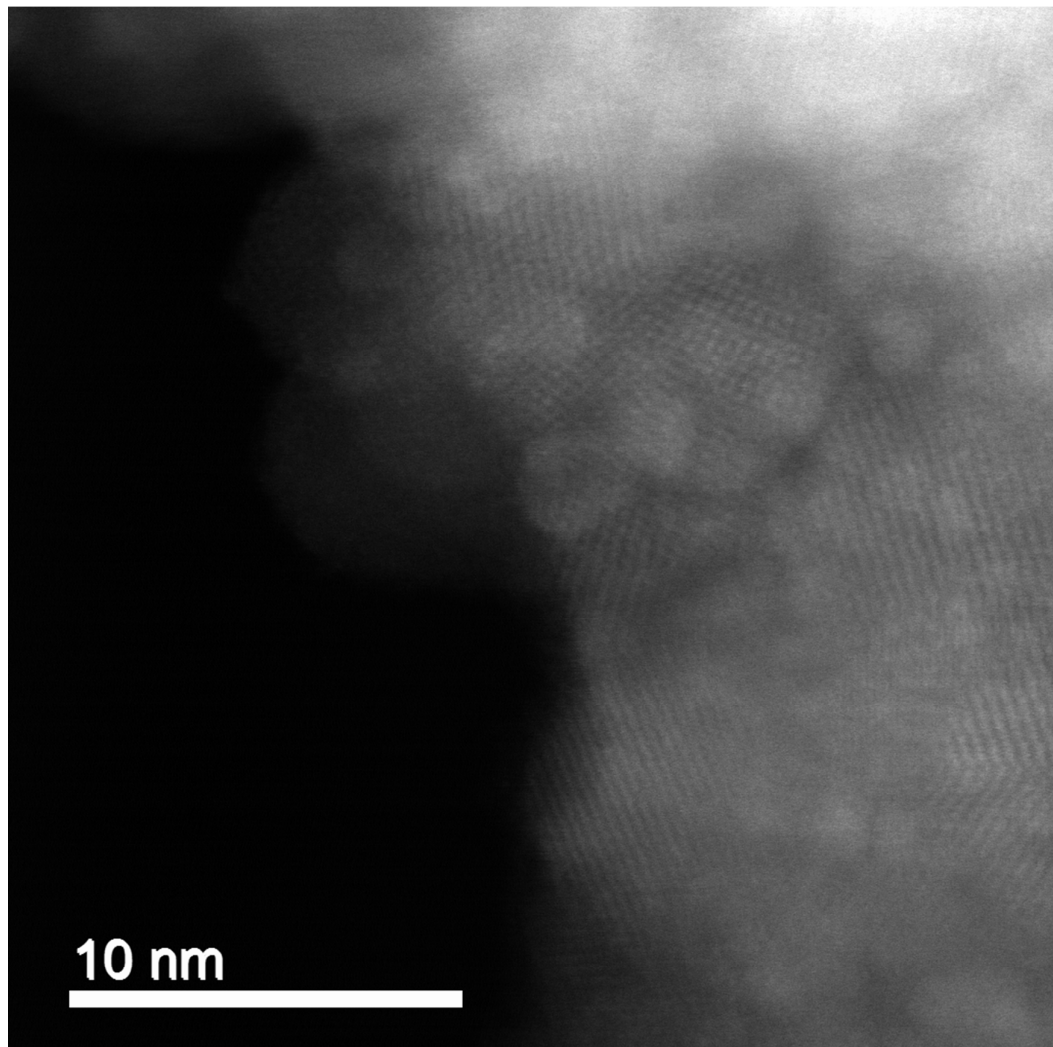
Figure S2



Graphic output of the WPPM modelling of **SBC1** (black open squares are observed data, red continuous line the calculated data, and the lower blue continuous line is the difference curve between observed and calculated profiles).

*Supplementary Information File*

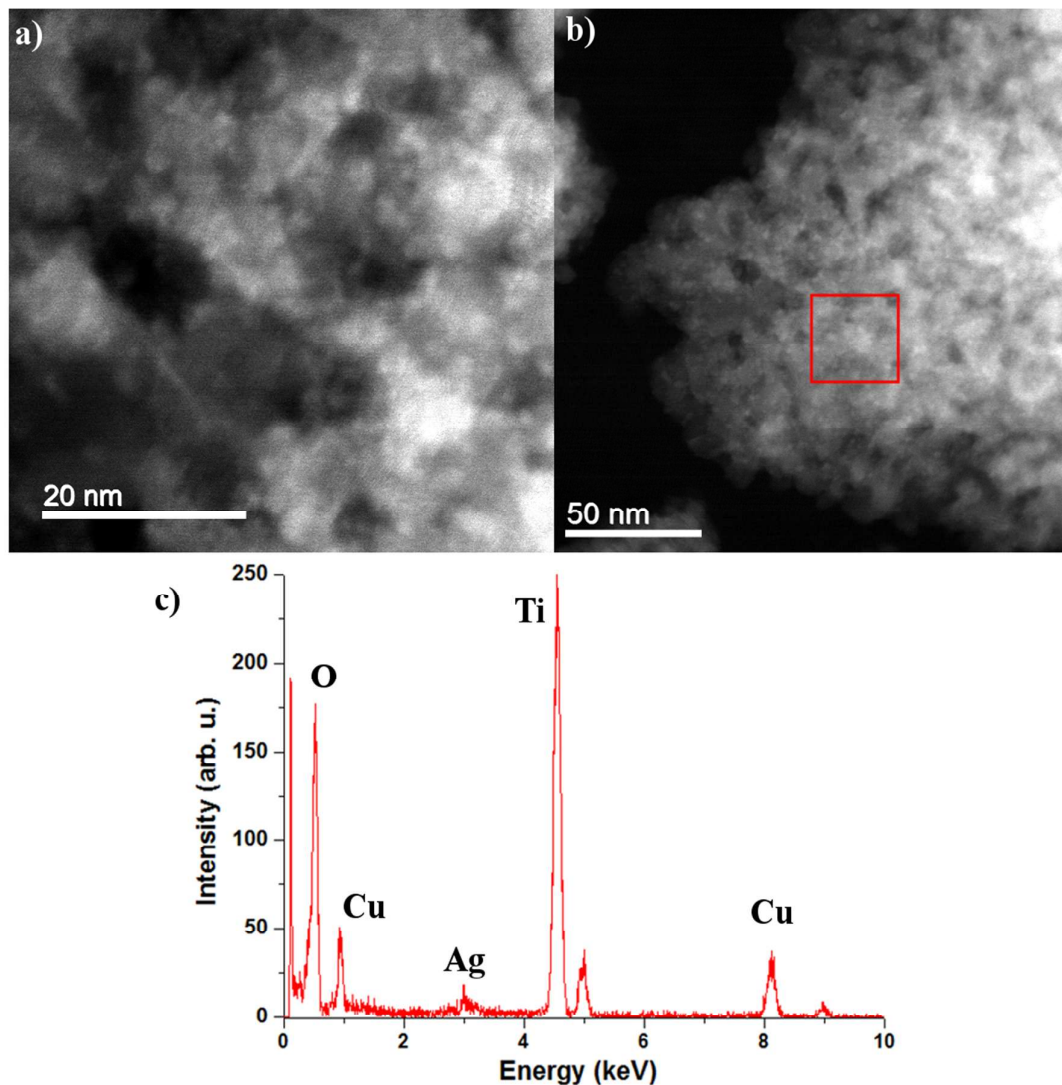
Figure S3



HR-STEM HAADF micrograph of  $\text{TiO}_2$  NPs.

*Supplementary Information File*

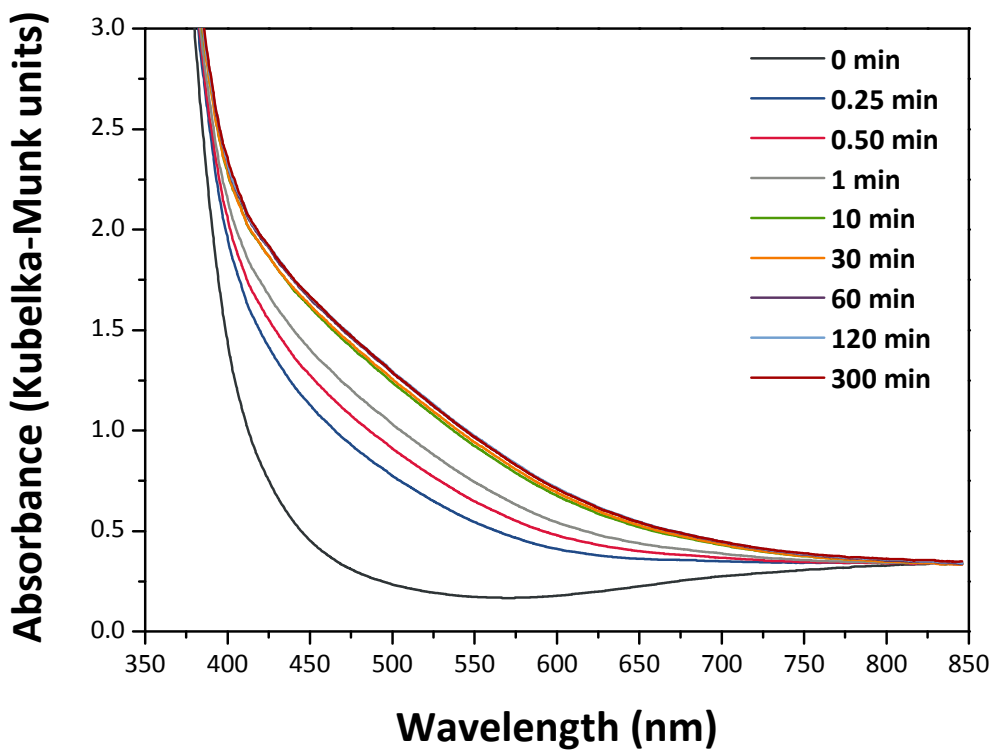
Figure S4



a) HR-STEM-HAADF micrograph of sample **SBC10**. b) Low magnification STEM-HAADF micrograph of the sample **SBC10**. The red square highlights the area used to acquire the EDS spectrum in c), rastering the beam in this region.

*Supplementary Information File*

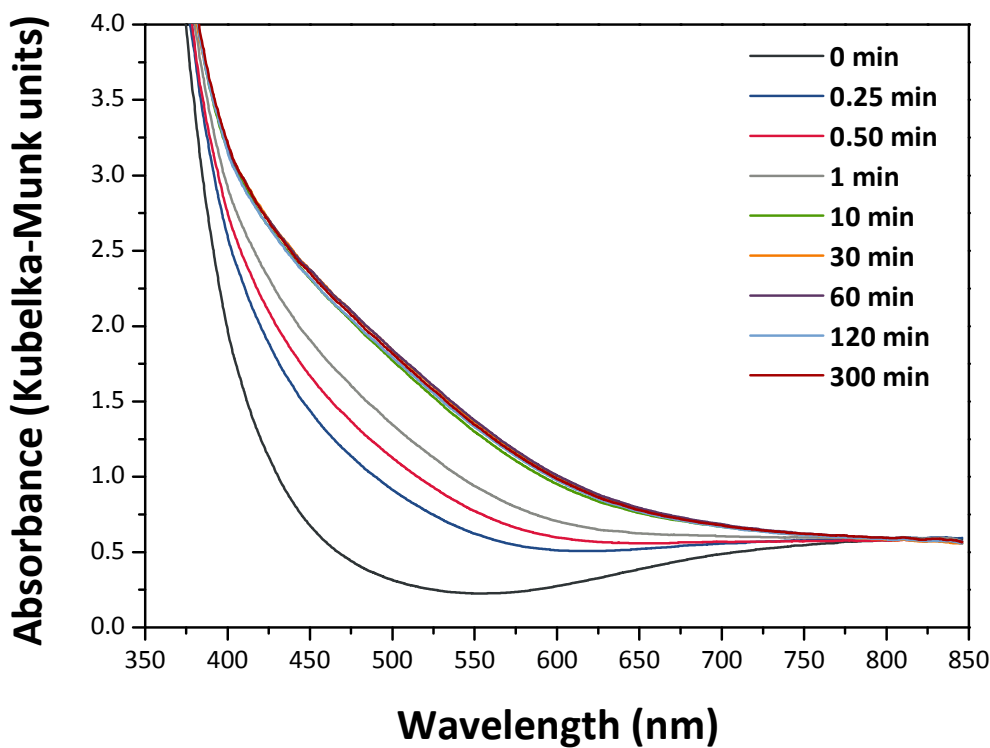
Figure S5a



DRS spectra of sample **SBC1** irradiated with UVA-light for 0, 0.25, 0.50, 1, 10, 30, 60, 120 and 300 min.

*Supplementary Information File*

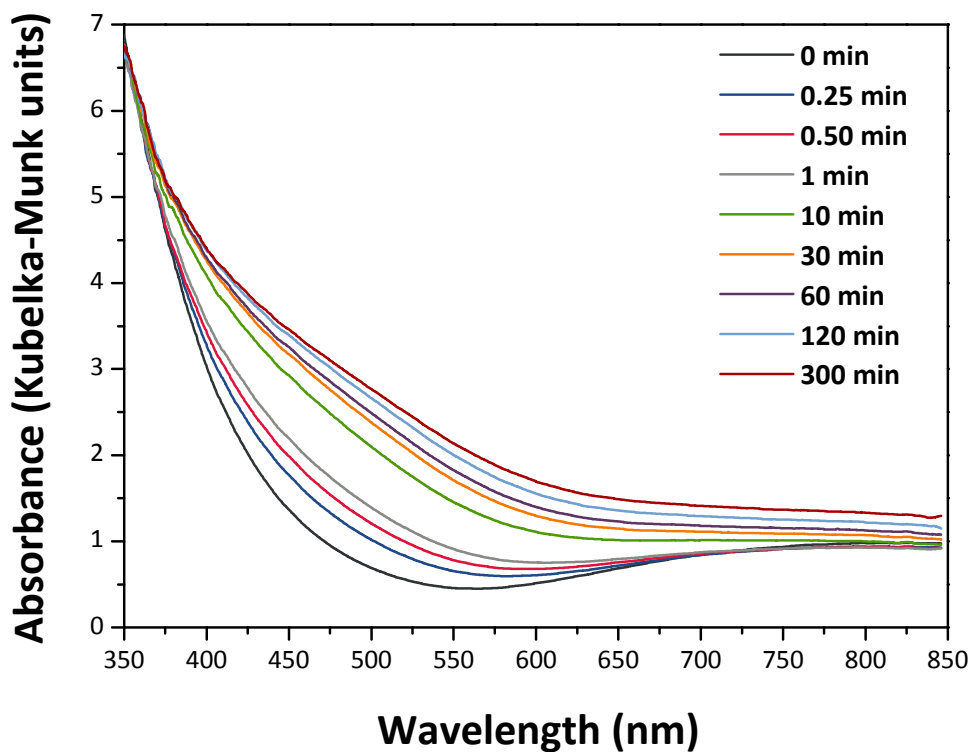
Figure S5b



DRS spectra of sample **SBC2** irradiated with UVA-light for 0, 0.25, 0.50, 1, 10, 30, 60, 120 and 300 min.

*Supplementary Information File*

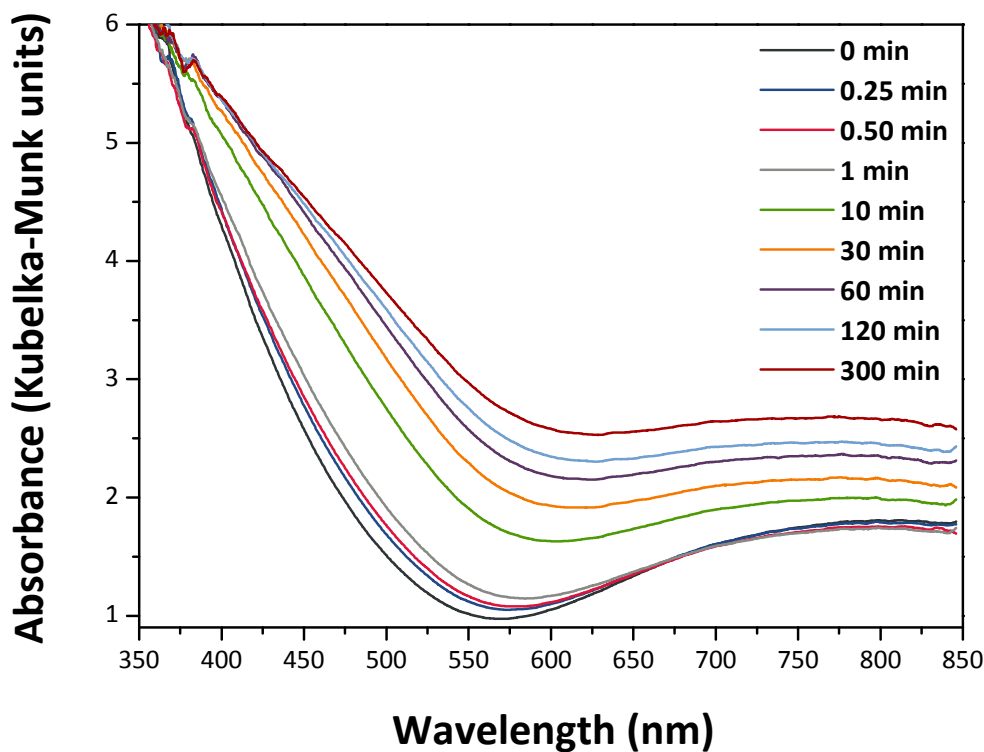
Figure S5c



DRS spectra of sample **SBC5** irradiated with UVA-light for 0, 0.25, 0.50, 1, 10, 30, 60, 120 and 300 min.

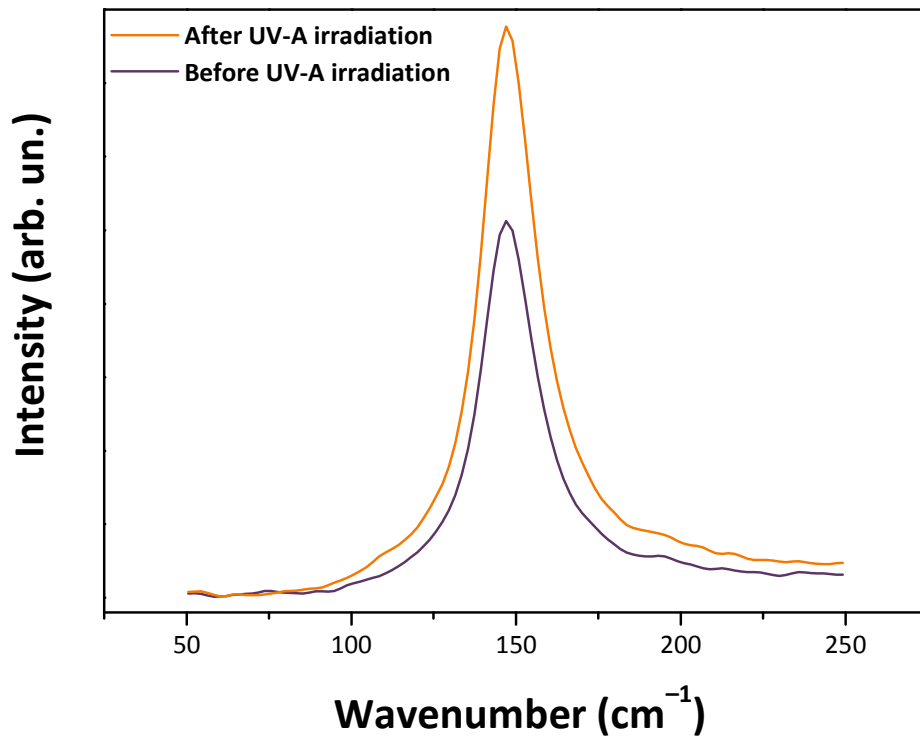
*Supplementary Information File*

Figure S5d



DRS spectra of sample **SBC10** irradiated with UVA-light for 0, 0.25, 0.50, 1, 10, 30, 60, 120 and 300 min.

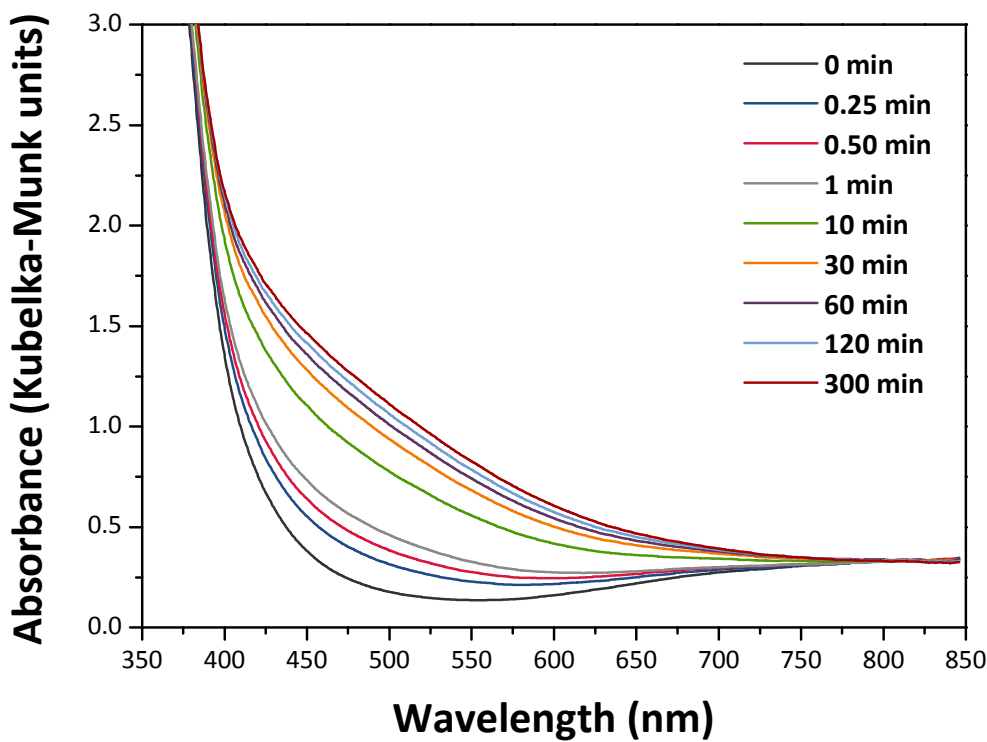
Figure S6



Raman spectra (in the 50–250  $\text{cm}^{-1}$  wavenumber region, to highlight the Raman  $E_g$  mode of anatase) of un-irradiated **SBC5**, and of the same specimen after being irradiated for 300 min with the UV-A lamp.

*Supplementary Information File*

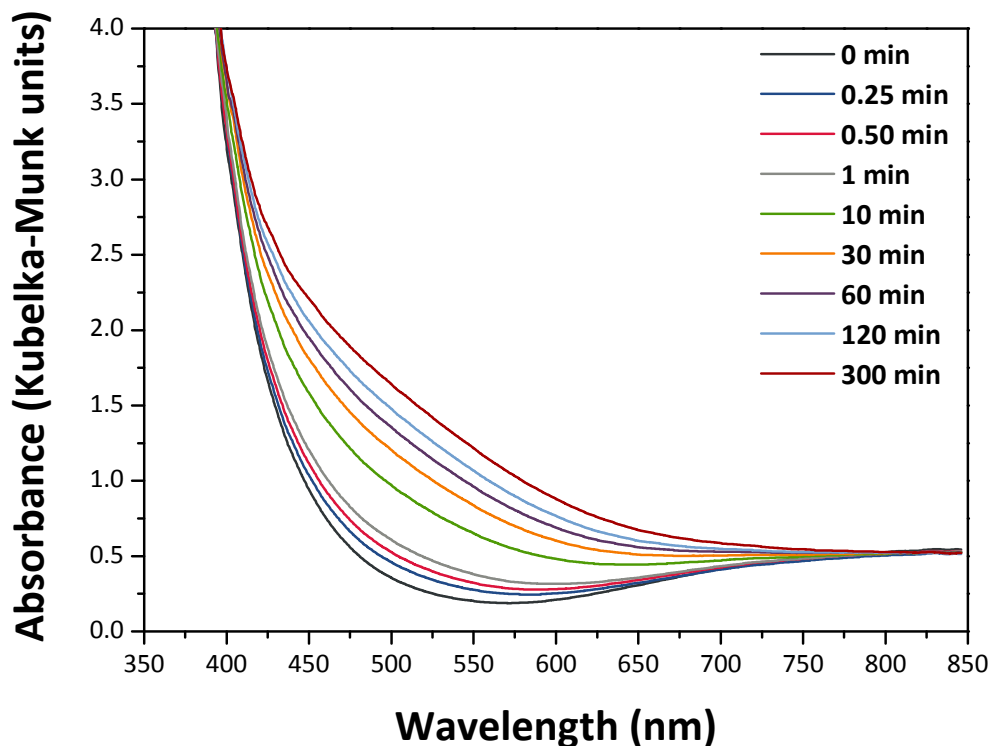
Figure S7a



DRS spectra of sample **SBC1** irradiated with vis-light for 0, 0.25, 0.50, 1, 10, 30, 60, 120 and 300 min.

*Supplementary Information File*

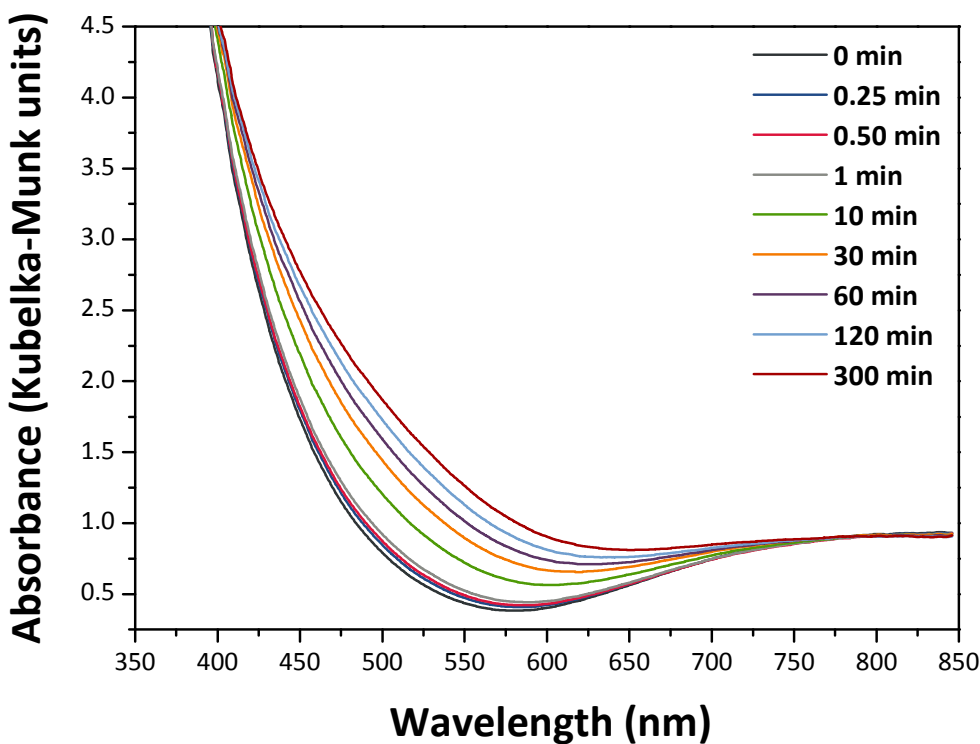
Figure S7b



DRS spectra of sample **SBC2** irradiated with vis-light for 0, 0.25, 0.50, 1, 10, 30, 60, 120 and 300 min.

*Supplementary Information File*

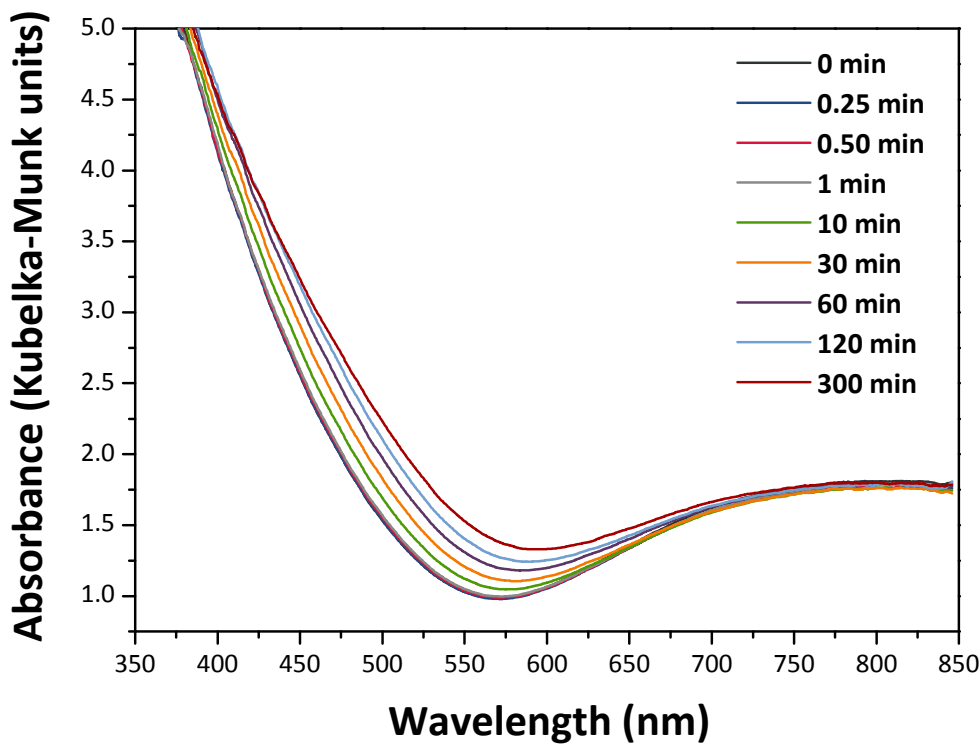
Figure S7c



DRS spectra of sample **SBC5** irradiated with vis-light for 0, 0.25, 0.50, 1, 10, 30, 60, 120 and 300 min.

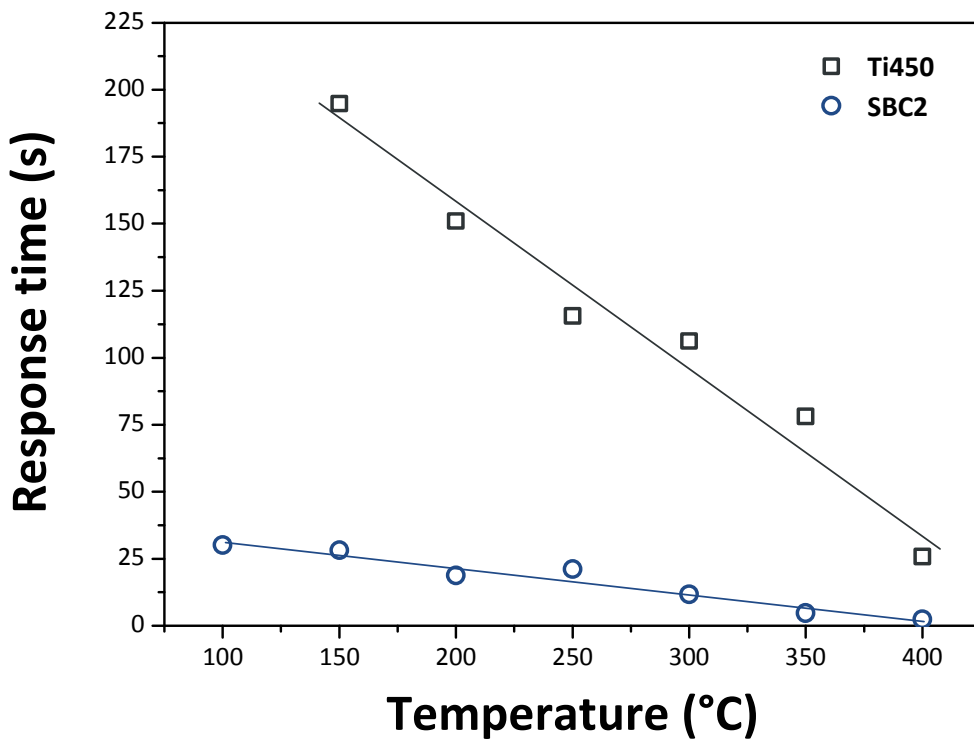
*Supplementary Information File*

Figure S7d



DRS spectra of sample **SBC10** irradiated with vis-light for 0, 0.25, 0.50, 1, 10, 30, 60, 120 and 300 min.

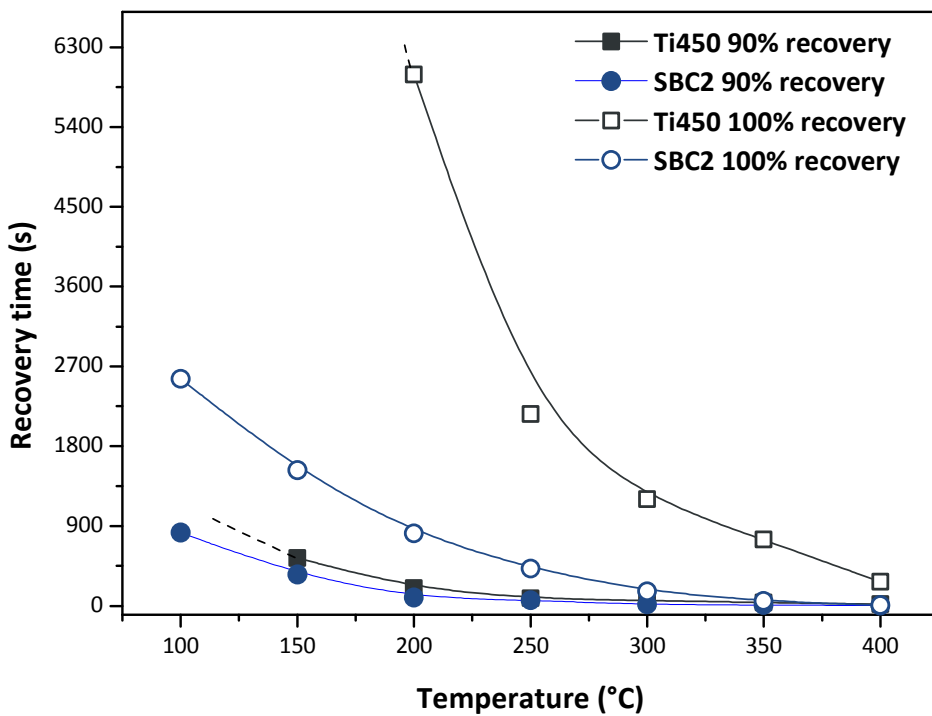
Figure S8a



Response time at 90% signal variation as function of temperature towards 20 ppm acetone of **Ti450** and **SBC2** based sensors

*Supplementary Information File*

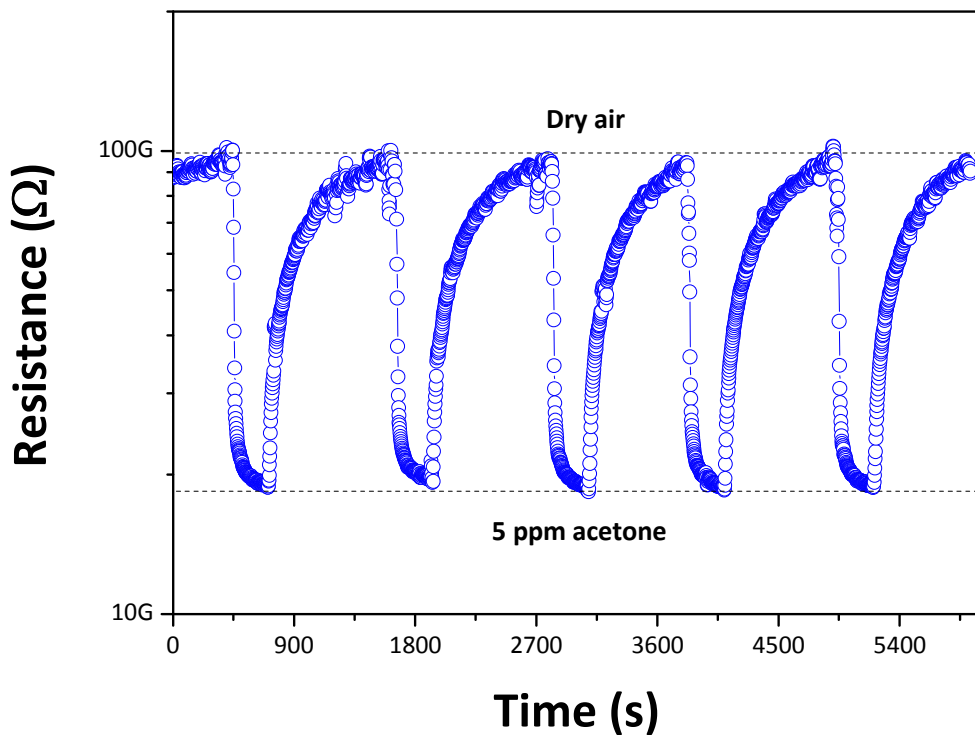
Figure S8b



Recovery times at 90% and 100% of the baseline signal recovery respectively, as function of temperature after exposure to 20 ppm acetone of **Ti450** and **SBC2** based sensors

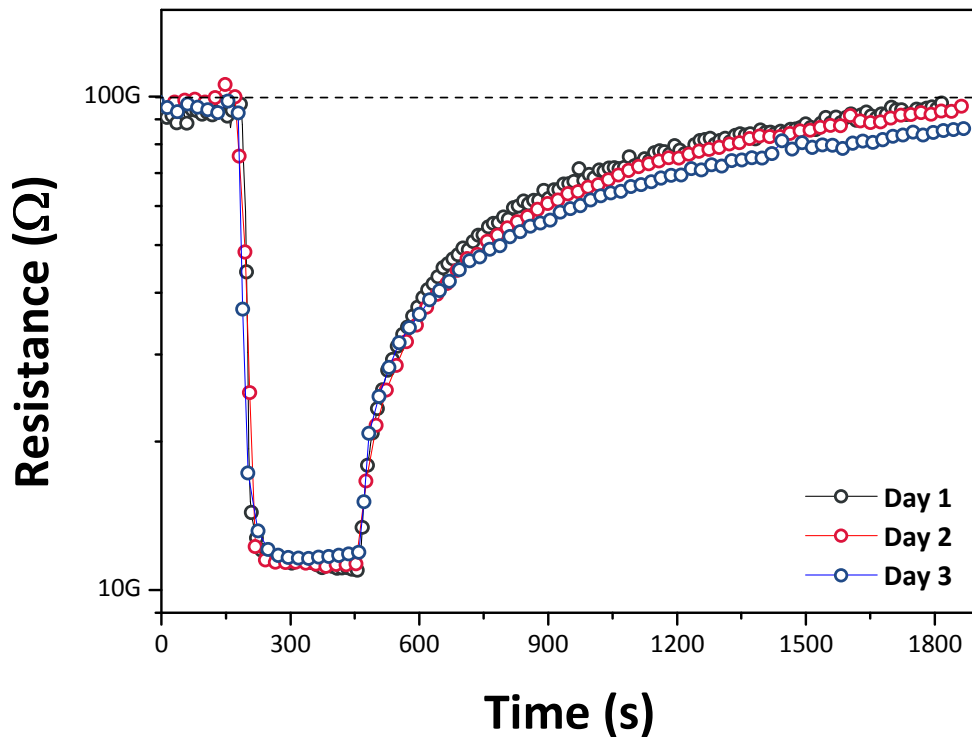
*Supplementary Information File*

Figure S9a



Reproducibility of response during five consecutive exposures to 5 ppm of acetone in dry air of **SBC2** based sensor

Figure S9b



Reproducibility of response to 20 ppm acetone in dry air, recorded during three different days, of **SBC2** based sensor

***Supplementary Information File***

Table S1 – Position and FWHM of Raman  $E_g$  mode of anatase.

Sample	Anatase Raman $E_g$ mode ( $\text{cm}^{-1}$ )	
	Position	FWHM
<b>Ti450</b>	145.1±0.1	15.4±0.6
<b>SBC1</b>	145.3±0.1	15.7±0.4
<b>SBC2</b>	146.3±0.1	16.9±0.4
<b>SBC5</b>	147.8±0.1	20.0±0.7
<b>SBC10</b>	148.1±0.1	21.4±0.8